This file was created by scanning the printed publication. Text errors identified by the software have been corrected: however, some errors may remain.

Labile dissolved organic carbon supply limits hyporheic denitrification

Jay P. Zarnetske,[1,2] Roy Haggerty,[3] Steven M. Wondzell,[4] and Michelle A. Baker[5]

Received 4 April 2011; revised 11 October 2011; accepted 22 October 2011; published 31 December 2011.

[1] We used an in situ steady state ^{15}N-labeled nitrate ($^{15}NO_3^-$) and acetate (AcO^-) well-to-wells injection experiment to determine how the availability of labile dissolved organic carbon (DOC) as AcO^- influences microbial denitrification in the hyporheic zone of an upland (third-order) agricultural stream. The experimental wells receiving conservative (Cl^- and Br) and reactive ($^{15}NO_3^-$) solute tracers had hyporheic median residence times of 7.0 to 13.1 h, nominal flowpath lengths of 0.7 to 3.7 m, and hypoxic conditions (<1.5 mg O_2 L^{-1}). All receiving wells demonstrated $^{15}N_2$ production during ambient conditions, indicating that the hyporheic zone was an environment with active denitrification. The subsequent addition of AcO^- stimulated more denitrification as evidenced by significant $\delta^{15}N_2$ increases by factors of 2.7 to 26.1 in receiving wells and significant decreases of NO_3^- and DO in the two wells most hydrologically connected to the injection. The rate of nitrate removal in the hyporheic zone increased from 218 kg ha^{-1} yr^{-1} to 521 kg ha^{-1} yr^{-1} under elevated AcO^- conditions. In all receiving wells, increases of bromide and $^{15}N_2$ occurred without concurrent increases in AcO^-, indicating that 100% of AcO^- was retained or lost in the hyporheic zone. These results support the hypothesis that denitrification in anaerobic portions of the hyporheic zone is limited by labile DOC supply.

Citation: Zarnetske, J. P., R. Haggerty, S. M. Wondzell, and M. A. Baker (2011), Labile dissolved organic carbon supply limits hyporheic denitrification, *J. Geophys. Res.*, *116*, G04036, doi:10.1029/2011JG001730.

1. Introduction

[2] There are many environments where denitrification occurs, but studies have shown that stream systems are particularly efficient at removing and retaining excess nitrogen (N) [*Seitzinger et al.*, 2006] with headwater and midnetwork streams being the most effective in regulation of downstream N exports [*Peterson et al.*, 2001; *Alexander et al.*, 2000; *Mulholland et al.*, 2008]. Characteristic of these headwater and midnetwork streams is the prominence of stream water–groundwater (hyporheic) exchange flux relative to surface water flux [*Anderson et al.*, 2005], especially during periods of low discharge [*Wondzell*, 2011]. Hyporheic exchange is also known to strongly influence N transformations and cycling in streams by increasing solute residence times and solute contact with reactive biofilms [*Duff and Triska*, 1990; *Holmes et al.*, 1994; *Jones*, 1995; *Wondzell and Swanson*, 1996; *Valett et al.*, 1996; *Hedin et al.*, 1998; *Hill et al.*, 1998]. Therefore, it follows that hyporheic exchange can exert a primary hydrologic control on the export of N from small to midnetwork watersheds.

[3] A key factor in the fate of N traveling through a hyporheic zone (Figure 1) is the organic carbon (C) conditions (substrate quality and quantity) in the stream and hyporheic zone [*Baker et al.*, 1999; *Kaplan and Newbold*, 2000; *Sobczak and Findlay*, 2002]. In streams, the predominant form of C is dissolved organic carbon (DOC) [*Fisher and Likens*, 1973] and only a fraction of that DOC is readily labile (i.e., bioavailable) [*Swank and Caskey*, 1982]. For hyporheic systems, either surface or groundwaters enriched with DOC are advected into hyporheic systems and fuel aerobic and anaerobic hyporheic metabolism [*Findlay*, 1995; *Jones*, 1995; *Baker et al.*, 2000].

[4] As reviewed by *Duff and Triska* [2000, and references therein], the occurrence of denitrification in the hyporheic zone is complex and is not just related to DOC and NO_3^- availability. Denitrification along hyporheic flowpaths is also a function of (1) the concentration of DO across the hyporheic zone which is controlled by biochemical oxygen demand and advected supply; (2) hyporheic water temperature because it controls microbial activity and DO saturation in water; and (3) the hydraulics that drive the physical transport and residence time of water such as the head gradient, hydraulic conductivity, advection, and dispersion. Of these factors,

[1]Department of Geosciences and Water Resources Graduate Program, Oregon State University, Corvallis, Oregon, USA.
[2]Now at School of Forestry and Environmental Studies, Yale University, New Haven, Connecticut, USA.
[3]Department of Geosciences and Institute for Water and Watersheds, Oregon State University, Corvallis, Oregon, USA.
[4]Pacific Northwest Research Station, Olympia Forestry Sciences Laboratory, Olympia, Washington, USA.
[5]Department of Biology and the Ecology Center, Utah State University, Logan, Utah, USA.

Copyright 2011 by the American Geophysical Union.
0148-0227/11/2011JG001730

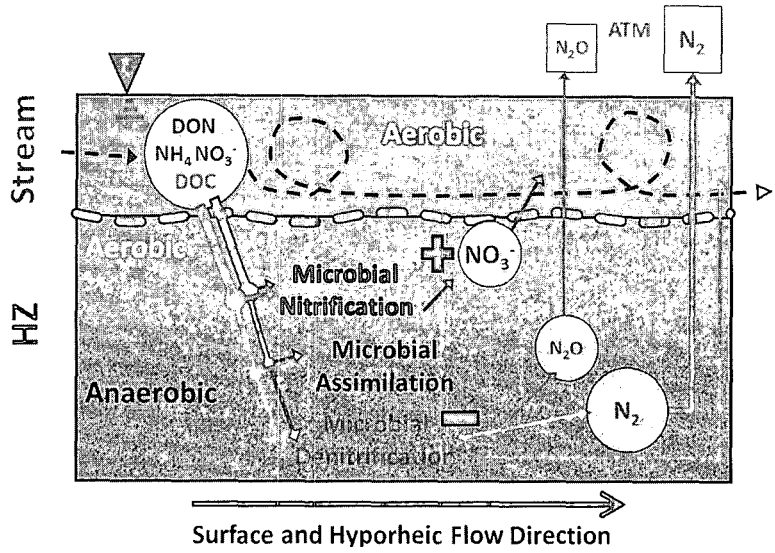

Figure 1. Illustration showing a simplified longitudinal cross-sectional view of a stream hyporheic (HZ) environment with commonly observed microbially mediated pathways for nitrate (NO_3^-) transformations. These pathways were observed in the present study's hyporheic system [*Zarnetske et al.*, 2011]. Surface waters supply NO_3^- and dissolved organic nitrogen (DON) and carbon (DOC) to the hyporheic zone. In aerobic regions of the hyporheic zone, DON can be mineralized to NH_4^+, which can be transformed via nitrification to create additional NO_3^-. The DOC and NO_3^- also can be retained in the hyporheic zone via microbial assimilation processes. DOC and NO_3^- entering anaerobic portions of the hyporheic zone can be utilized for denitrification, which produces dinitrogen oxide (N_2O) and dinitrogen (N_2). The N_2O and N_2 can degas out of the stream system and return to the atmosphere (ATM).

the biogeochemical conditions controlling hyporheic denitrification primarily vary by the amount of NO_3^- and quality and quantity of DOC present in the system [*Findlay*, 1995; *Kaplan and Newbold*, 2000]. If both NO_3^- and labile DOC are abundant then denitrification rates can be large [e.g., *Holmes et al.*, 1996, *Storey et al.*, 2004]. Spatial patterning of DOC availability along hyporheic flowpaths adds further to the complexity. DOC and DO are expected to decline at the head of the hyporheic flowpaths as microbial processes preferentially utilize DO and labile fractions of DOC [*Vervier and Naiman*, 1992; *Sobczak et al.*, 2003; *Zarnetske et al.*, 2011]. Further along the hyporheic flowpaths the labile DOC availability can become depleted leading to DOC quality limitations on denitrification [*Sobczak et al.*, 2003; *Zarnetske et al.*, 2011]. Also, hyporheic DOC sources from stream and groundwater vary with discharge and season [*Vervier and Naiman*, 1992; *Baker and Vervier*, 2004] which, in turn, vary hyporheic metabolism and denitrification.

[5] The use of stable isotope (^{15}N) tracers has greatly advanced understanding of aquatic N cycling by allowing the tracing of N through ecosystem pathways experiencing different physical and biological conditions. For example, *Böhlke et al.* [2004] and *Mulholland et al.* [2004, 2008] demonstrated the usefulness of the ^{15}N tracer approach for estimating denitrification rates of streams at the reach scale. More recently, subsurface ^{15}N tracing has been successfully used to study hyporheic processes associated with reactive N transport [*Clilverd et al.*, 2008; *Böhlke et al.*, 2009; *Zarnetske et al.*, 2011]. Direct hyporheic ^{15}N addition enables the distinction between microbial assimilation and retention pathways and the respiratory denitrification pathway (i.e., microbial N_2 production), which was not possible in previous hyporheic coupled C-N studies that relied on C and N mass balance approaches [e.g., *Hedin et al.*, 1998; *Baker et al.*, 1999; *Sobczak et al.*, 2003]. On the other hand, previous studies have directly measured hyporheic denitrification (via acetylene block, N_2:Ar ratios, or $^{15}NO_3^-$ additions) across spatial and temporal ranges of DOC and NO_3^- conditions and found that a positive correlation exists between the quantity of labile DOC and N_2O production [*Baker and Vervier*, 2004; *Smith et al.*, 2006; *Arango et al.*, 2007; *Böhlke et al.*, 2009]. Though the previous studies on coupled hyporheic DOC and N dynamics consistently indicate that the type and quality of DOC in a hyporheic system influences denitrification rates, none have both isolated the role of labile DOC supply on denitrification and made direct measurements in a hyporheic environment.

[6] We evaluate the role of labile DOC on denitrification along a redox gradient that forms along hyporheic flowpaths in a gravel bar. We combined $^{15}NO_3^-$ tracing techniques with an addition of labile DOC to examine the role of DOC in controlling denitrification. The previous work at this study site demonstrated that denitrification and DOC dynamics were closely coupled [*Zarnetske et al.*, 2011]. Under base flow conditions, DOC persisted across all residence times, but denitrification rates and DOC uptake decreased beyond threshold flowpath lengths and residence times (solid curves in Figure 2). Further, labile DOC was preferentially lost at the heads of hyporheic flowpaths, leaving the less labile fraction to be transported to more distal portions of the

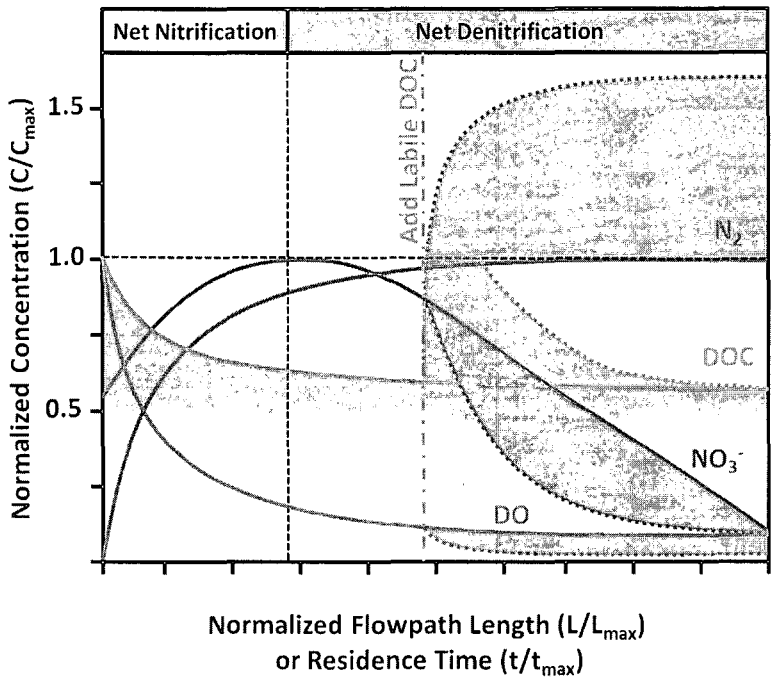

Figure 2. Steady state denitrification dynamics at the study site hyporheic zone (solid curves, modified from *Zarnetske et al.* [2011]) showing the hypothesized response of denitrification (dashed curves) to an addition of labile dissolved organic carbon (DOC). The shaded regions represent a net change in the abundance of a solute due to the addition of labile DOC. Note that the labile fraction of the total DOC is presented as the upper shaded region under the DOC curve with the remainder of the mass representing less bioavailable forms of DOC. Overall, we hypothesize that the addition of labile DOC to the hyporheic zone will significantly increase dinitrogen (N_2) production, decrease total nitrate (NO_3^-) concentration and mass transported through the system, and facilitate additional dissolved oxygen (DO) consumption.

flowpath [*Zarnetske et al.*, 2011]. Based on our previous results [*Zarnetske et al.*, 2011], we hypothesized that denitrification in this hyporheic zone is limited by the amount of labile DOC supplied to the hypoxic-anoxic portions of the hyporheic zone. We expected that adding labile DOC to the middle of these hyporheic flowpaths would increase metabolic processing rates downgradient of the addition such that DO will decrease, N_2 production would increase, and overall NO_3^- mass export would decrease (dashed curves in Figure 2).

2. Methods

2.1. Study Site

[7] The study site is a gravel bar in Drift Creek (Figure 3a), a third-order stream in the Willamette River basin in western Oregon, USA (44.9753°N, 122.8259°W). The drainage basin is 6517 ha, and has mixed land use dominated by agriculture (lower catchment) and forestry (upper catchment). The basin's population is primarily rural and residences are serviced by septic systems, another potential source of N in the study stream. Annual precipitation is 1190 mm and comes predominantly during the winter as rain. Base flow discharge gradually decreases to an annual minimum (<50 L s^{-1}) in early September. The study reach was modified by channelization in the past, as were many of the streams in this agricultural region. The channelized stream is incised into competent bedrock (andesite flow breccias) and is now separated from its floodplain. The active channel is 5–20 m wide and is bounded by steep banks 3–5 m high. The alluvial thickness above bedrock (as depth to refusal) varies from 0 to ≥1.5 m, which constrains the extent of the hyporheic zone. The study reach has a slope of 0.007 m m^{-1} and the morphology is primarily a planebed channel with occasional pool-riffle sequences (see *Montgomery and Buffington* [1997] for definitions of channel types). The streambed and gravel bar consists of poorly sorted sand, gravel, cobbles, and boulders.

[8] The hyporheic zone study site is a lateral gravel bar approximately 6.1 m by 4 m (Figure 3b) with a riffle on one side and connected to the bedrock channel bank on the other side. The gravel bar separates two pools and spans a head loss across the riffle of 0.135 m. The alluvium comprising this gravel bar was uniformly 1.2 m thick. This gravel bar was instrumented with a well network (n = 11) of 3.8 cm I.D. schedule 40 PVC wells screened 0.2–0.4 m below ground surface. The observed and modeled subsurface exchange across this gravel bar primarily occurs along lateral flowpaths from the head to the tail of the bar (Figure 3b). A previous investigation demonstrated that all wells are connected to stream water and that well waters come from the stream and not the local groundwater aquifer [*Zarnetske et al.*, 2011]. Based upon multiple tracer tests at the study site, the hydraulic conductivity of the gravel bar is 4.03 to 6.63 m d^{-1}.

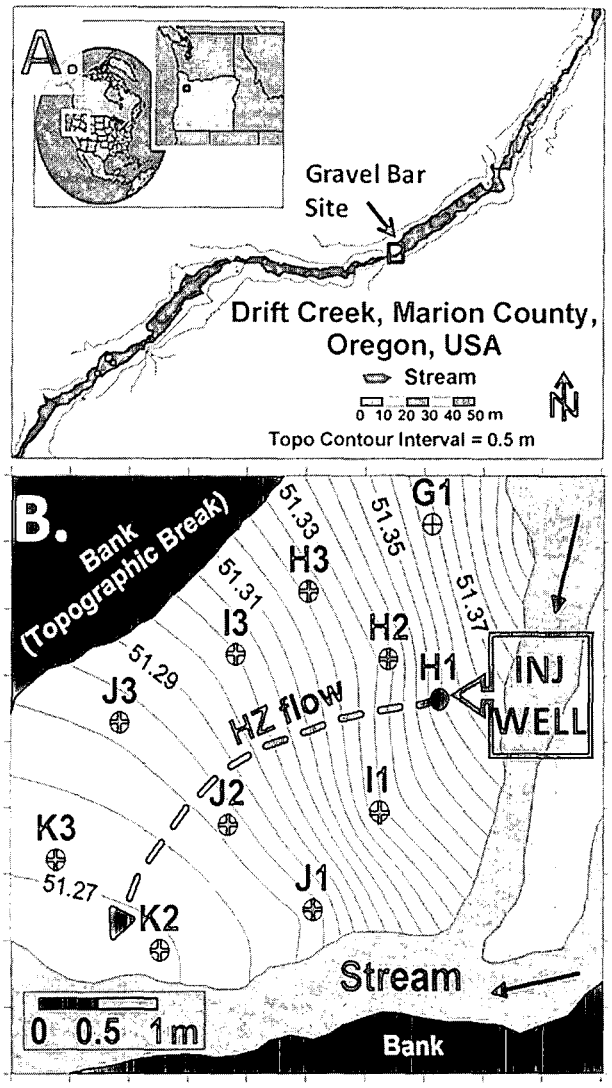

Figure 3. (a) Map of the Drift Creek study site showing lateral gravel bar hyporheic site. (b) Map of the hyporheic study site showing locations of wells (dots with cross hairs), hyporheic injection site, and water potentiometic surface during the injection experiment. Note that the stream briefly bifurcates near the gravel bar (i.e., not a tributary confluence) and water chemistry is the same across the channel. Dotted arrow indicates a single representative simulated advective flowpath from the injection well (H1) to the stream.

2.2. Tracer Experiment

[9] A 48 h steady state well injection of a conservative tracer, Cl^-, and, $^{15}NO_3^-$ was used to quantify ambient hyporheic denitrification via $^{15}N_2$ production. Following ambient plateau measurements of denitrification during the first 24 h, a second conservative tracer, Br^-, and labile DOC source, acetate (AcO^-), were coinjected for an additional 24 h to measure hyporheic denitrification under increased labile DOC supply. AcO^- was selected because (1) it is naturally produced and consumed in many aquatic systems, including hyporheic zones [*Chapelle and Bradley*, 1996; *Baker et al.*, 1999], (2) it is highly bioavailable to microbes [*Drake*, 1994], (3) it is highly soluble (NaAcO solubility at 20°C = 464 g L^{-1}), and (4) has demonstrated low sorption potentials in natural stream sediments (e.g., $K_d \approx 0$ [*Baker et al.*, 1999]). Further, AcO^- was used as a pure DOC source so as to avoid the confounding factor of using more complex natural DOC sources (e.g., leaf leachate) which contains additional nutrients [*Sobczak et al.*, 2003].

[10] The injection experiment was performed on 1–3 September 2008 when stream discharge and hyporheic head gradients were stable. The injection consisted of two steady state experimental periods: "Pre-DOC" and "DOC." During the Pre-DOC period, an injection solution of $^{15}NO_3^-$ (as 99% enriched $K^{15}NO_3^-$) and Cl^- (as $NaCl^-$) was released at a constant rate (3 mL min^{-1}) using a metering pump (FMI QG150, Fluid Metering, Inc., Syosset, NY, USA; note that the use of trade names in this publication is for reader information and does not imply endorsement by the U.S. Department of Agriculture of any product or service) into the upgradient injection well, H1, for 47.75 h starting at 14:45 on 1 September. During the DOC period, an injection solution of conservative tracer Br^- (as KBr) and NaAcO was released at a constant rate (6 mL min^{-1}) into H1 with a second FMI QG150 metering pump for 21.17 h starting at 17:20 on 2 September.

[11] Based upon pilot studies of dilution factors between the injection site and the downgradient receiving wells, the injected solutes needed to be substantially more concentrated than the ambient hyporheic conditions. The $^{15}NO_3^-$ introduced at the injection site, H1, had a concentration of 30.7 mg L^{-1}, which was calculated to produce a maximum hyporheic $\delta^{15}N$ enrichment plume of 40,000‰ in the hyporheic water NO_3^- leaving the injection site. The Cl^- injection concentration was 4,367 mg L^{-1} based upon an addition target to elevate the background hyporheic Cl^- by 1,260% and generate clearly detectable specific conductivity (SC) increase in downgradient hyporheic flowpaths. The AcO^- injection concentration was 504 mg L^{-1}, while the Br^- injection concentration was 50 mg L^{-1}. During the entire injection time, the injection well water column was continually mixed via closed system peristaltic pumping to ensure full solute mixing and equal concentration release across the entire screened well section (0.2–0.4 m below ground surface). The low injection pump rates during the experiment did not create a detectable increase in head elevation in well H1. The injection solution had an O_2 concentration of 4.4 mg O_2 L^{-1} during the injection, which matches the ambient O_2 concentration observed at H1 prior to the start of the injection. We did not observe a change in the O_2 concentration at the injection site during the experiment.

[12] We used specific conductivity to measure the real-time Cl^- transport between the source well and downgradient receiving wells. The specific conductivity measurements were taken every 60 s in 10 wells (H1, H2, H3, I1, I3, J1, J2, J3, K2, K3) and in the stream water at the head and tail of the gravel bar to detect if stream specific conductivity varied during the experiment. These specific conductivity measurements were made with 12 multiplexed, in situ, CS547A conductivity and temperature probes connected to a CR1000 (Campbell Scientific, Logan, Utah, USA). The specific conductivity measurements were used to characterize the conservative solute transport dynamics including flow rates, flow

paths, and residence times as well as to inform the timing of the sampling regime described below (for additional detail, see *Zarnetske et al.* [2011]).

[13] The water sampling regime consisted of collecting multiple rounds of hyporheic samples during the three phases of the experiment: (1) Preinjections, (2) Pre-DOC plateau ($^{15}NO_3^-$ and Cl^- steady state), and (3) DOC plateau (AcO^- and Br^- steady state). For each location (10 wells plus stream water at the gravel bar head), repeated sampling occurred during the preinjections (n = 3), Pre-DOC plateau (n = 5), and during DOC amendment (n = 5) periods. The Pre-DOC plateau sampling period was initiated at 18.5 h after $^{15}NO_3^-$ and Cl^- injection started when all hyporheic wells demonstrated steady state specific conductivity values. Following the Pre-DOC Cl^- transport times, the DOC amendment sampling period was initiated at 18.5 h after AcO^- and Br^- injected started. Repeated hyporheic samples were collected approximately every ~2 h during each respective plateau period. All samples were analyzed for solutes relevant to denitrification and tracing injection solutes ($\delta^{15}NO_3^-$, $\delta^{15}N_2$, as well as concentrations of NO_3^-, AcO^-, total DOC, DO, Cl^-, and Br^-). Hydraulic transport parameters (head, flow rates, flowpaths, and residence times) were also measured along the instrumented hyporheic zone.

[14] Hyporheic well samples were collected with a field peristaltic pump (Masterflex L/S, Vernon Hills, Illinois, USA) [*Woessner*, 2007]. All water samples were immediately filtered through ashed Whatman GF/F glass fiber filters (0.7 μm pore size) into acid washed HDPE bottles (60 mL for nutrient chemistry and 1 L for $\delta^{15}N$ isotope samples). Following filtering, nutrient chemistry samples and isotope samples were stored on ice in the field and later refrigerated at 4°C or frozen in the laboratory until processed and analyzed. DO concentrations were measured in situ with a calibrated YSI DO Meter (Model 52) at all locations prior to collecting each round of samples. Samples were also collected for $\delta^{15}N_2O$ (g), but could not to be analyzed due to technical problems at the stable isotope laboratory. Nonetheless, denitrification in freshwater and nearshore marine system sediments consists almost entirely of N_2 production with N_2O/N_2 production ratios generally between <0.001 and <0.05 [*Seitzinger*, 1988; *Mulholland et al.*, 2004], so $\delta^{15}N_2$ by itself is capable of characterizing the majority of the denitrification dynamics.

[15] The $\delta^{15}N$ gas collection for each sample occurred in the field and followed procedures adapted from *Hamilton and Ostrom* [2007]. A low-flow peristaltic pump was used to collect 80 mL water samples into a 140 mL plastic syringe (Becton-Dickinson, Franklin Lakes, NJ, USA) fitted with stopcocks. All detectable bubbles were expelled to create a zero headspace. Sample syringes were submerged under water in a processing tub kept at stream temperature to avoid atmospheric N contamination. An underwater transfer of 40 mL high-purity He was added to each sample syringe. Equilibration of the N_2 (g) into the He headspace of each sample was achieved by gently agitating the syringes for 10 min. After equilibration, 14 mL of headspace gas was injected into preevacuated 12 mL exetainers (Labco Ltd., Wycombe, UK). Preevacuation of exetainers was achieved by pumping them down to a pressure of <50 mTorr using a Welch vacuum pump (Model DirectTorr 8905, Skokie, Illinois, USA). All exetainers were stored underwater in He purged DI water-filled centrifuge tubes until sample collection. All sample-filled exetainers were returned to their zero headspace He purged DI water-filled centrifuge tubes for storage until analysis.

[16] We conducted a detailed survey of surface water elevations and channel topography around the instrumented gravel bar using a Topcon total station (Model GTS-226, Livermore, California, USA) during the tracer experiment. The applied standard surveying methods had a spatial resolution of $x \leq 0.1$ m, $y \leq 0.1$ m, $z \leq 0.005$ m for the instrumented gravel bar.

2.3. Laboratory Procedures

[17] Stream and hyporheic samples were analyzed for NO_3^--N, DOC-C, AcO^- (CH_3COO^-), Cl^-, and Br^- at the Oregon State University Institute for Water and Watersheds Collaboratory (Corvallis, USA). The NO_3^--N measurements were made by a Technicon Auto-Analyzer II using standard colorimetric methodology with detection limits of 0.001 mg L^{-1}. The concentration of total DOC was determined with a Shimadzu TOC-VCSH Combustion Analyzer (Tokyo, Japan; detection limit = 0.05 mg L^{-1}). The AcO^-, Cl^-, and Br^- were determined by ion chromatography (Dionex 1500, Sunnyvale, California, USA; detection limit = 0.01 mg L^{-1}).

[18] The ^{15}N content of the stream and hyporheic water NO_3^- was determined by methods adapted from *Sigman et al.* [1997] and *Mulholland et al.* [2004]. These methods are briefly summarized below. Prior to ^{15}N analysis, $^{15}NO_3^-$ samples with blanks and standards were processed as follows: (1) A volume of each sample (0.25–1 L; processing volume is dependent on N content of each sample) was stripped of its dissolved NH_4^+ and had its NO_3^- concentrated; (2) the concentrated sample NO_3^- was captured on a prepared filter via a reduction/diffusion/sorption procedure (full reduction of NO_3^- to NH_4^+, which is then converted to NH_3 that diffuses into the headspace and ultimately gets captured on the acidified sorption filter); and (3) after complete transfer of NO_3^- to the sample filter, the samples were sealed and sent for $^{15}NO_3^-$ analysis. All $^{15}NO_3^-$ and ^{15}N-gas samples were analyzed by the Marine Biological Laboratory Stable Isotope Facility (MBL, Woods Hole, Massachusetts, USA). Data are reported using delta notation, where

$$\delta^{15}N = 1000 \times \left(\frac{R_{sample}}{R_{standard}} - 1\right) \quad (1)$$

and R is the ratio of ^{15}N:^{14}N in the sample or standard (atmospheric gas). Replicate analyses of the water and gas samples show the precision of $\delta^{15}NO_3^-$ and $\delta^{15}N_2$ isotope measurements is ±80.0‰ and ±0.2‰, respectively.

2.4. Parameter and Statistical Calculations

[19] The specific conductivity breakthrough curves (as a measure of Cl^- transport) were used to calculate the median residence time of the hyporheic water flowpaths for all downgradient wells receiving a detectable specific conductivity increase from the injection site. The median residence time was calculated as the time required to raise the specific conductivity in the well to one half the plateau specific conductivity [*Zarnetske et al.*, 2011]. The nominal flowpath

Table 1. Ambient Stream and Hyporheic Temperature and Biogeochemical Parameters and Nominal Transport Distance From the H1 Injection Site to Each Well[a]

Location	Temperature (°C)	DO (mg O_2 L^{-1})	NO_3^- (mg N L^{-1})	DOC (mg C L^{-1})	Acetate (mg AcO^- L^{-1})	Cl^- (mg L^{-1})	Br (mg L^{-1})	Nominal Distance From Injection[b] (m)
Stream	12.8	10.62	0.612	1.94	<0.01	3.596	0.011	−0.5
G1	13.1	4.24	0.433	1.54	<0.01	3.497	0.011	−1.54
H1 (injection site)	13.2	4.31	0.453	1.14	<0.01	3.485	0.010	0
H2	13.3	2.5	0.447	1.15	<0.01	3.528	0.014	+0.67
H3	13.8	0.83	0.37	0.85	<0.01	3.818	0.016	+1.5
I1	13.2	2.95	0.477	1.15	<0.01	3.537	0.013	+1.02
I3	13.8	0.88	0.394	0.91	<0.01	3.471	0.021	+1.75
J1	14.1	0.76	0.317	0.8	<0.01	3.421	0.018	+1.97
J2	14	0.88	0.413	0.84	<0.01	3.461	0.012	+2.18
J3	13.5	1.62	0.45	0.81	<0.01	3.500	0.012	+2.83
K2	14	0.7	0.348	0.76	<0.01	3.440	0.011	+3.12
K3	13.7	1.31	0.43	0.86	<0.01	3.479	0.010	+3.66

[a]Reported as means, $n = 3$.
[b]Plus and minus symbols denote upgradient and downgradient of H1, respectively.

length was measured as linear distance between the injection site and each downgradient well [*Zarnetske et al.*, 2011].

[20] The connectivity of the receiving wells to the injection well was based on the conservative tracer (Cl^- and Br^-) transport during the experiment. The hydrologic connectivity (D) to the injection well at steady state, i.e., the fraction of water arriving at the receiving well that originated at the injection, was calculated as:

$$D_{x,t} = \frac{C_{x,t} - C_{x,t=0}}{C_{inj} - C_{x,t=0}} \quad (2)$$

where c is the concentration of the conservative tracer Cl^-, x is the well location, t is the time of sample, and inj is the injection site. In the absence of biological or chemical removal pathways, conservative and reactive tracer transport should be identical. Based upon this assumption, we used the hydrologic connectivity, D, to calculate the predicted reactive solute concentrations for NO_3^-, DOC, and AcO^- in each of the receiving wells before and during the AcO^- augmentation period as:

$$S_{pred,x,t} = S_{inj}D_{x,t} + S_{x,t=0}(1 - D_{x,t}) \quad (3)$$

where S_{pred} is the predicted concentration of the solute of interest at steady state. We then calculated the difference between the measured and predicted reactive solute concentrations for each well during the AcO^- augmentation plateau conditions. NO_3^-, DOC, and AcO^- removal occurs when the observed concentration is less than the predicted concentration and production occurs when the observed concentration is greater than the predicted concentration [*Hedin et al.*, 1998; *Baker et al.*, 1999]. Further, if the difference between predicted and observed NO_3^- concentration increases following AcO^- augmentation, it indicates increased rates of NO_3^- removal along the hyporheic flowpath when AcO^- was added to the system.

[21] We compared changes in concentrations of solutes for the Pre-DOC and DOC treatment periods using a paired t test (significance at $p = 0.05$, df = 4). We treated repeated samples within a well as independent replicates. We ran paired t tests to determine how strongly means of Pre-DOC and means of DOC differed in each well. We excluded wells H3, I1, I3, J1, and J3 because they did not receive measureable concentrations of the added solutes.

3. Results

3.1. Background Stream and Hyporheic Biogeochemical Conditions

[22] Streamflow conditions were relatively stable over the experiment with a mean flow of 32 L s^{-1} and a variance of ±3.2 L s^{-1}. We did not observe any detectable change in head across the gravel bar during the experiment. Stream and hyporheic water temperature ranged between 12.8 and 15.8°C during the injection experiment. Measured stream surface water nutrient and chemistry conditions were stable during the experiment with mean and 1 standard deviation (n = 13) values of NO_3^- (0.61 ± 0.01 mg N L^{-1}), AcO^- (<0.01 ± 0.005 mg L^{-1}), DOC (1.94 ± 0.36 mg C L^{-1}), DO (10.62 ± 0.98 mg O_2 L^{-1}), Cl^- (3.60 ± 0.25 mg L^{-1}), Br^- (0.010 ± 0.005 mg L^{-1}) and pH (6.8 ± 0.2).

[23] Background hyporheic conditions collected immediately prior to the start of the injection experiment showed flow and biogeochemical conditions consistent with the previous study by *Zarnetske et al.* [2011]. Hyporheic flowpaths originated at the head of the gravel bar and are discharged to the stream at the tail of the gravel bar (Figure 3b). The biogeochemical conditions showed that the proximal ends of hyporheic flowpaths were characterized as oxic while distal ends were hypoxic and indicated net NO_3^- removal (Table 1). The supply of DOC and DO to the hyporheic zone was primarily from stream water advecting into the sediment at the head of the gravel bar (Figures 4e and 4g, respectively). The DO and DOC removal rates were greatest in the first 2 m of the hyporheic flowpaths, but removal persisted across the entire gravel bar. While the patterns were similar along the hyporheic flowpaths of the earlier study (solid curves in Figure 2) [*Zarnetske et al.*, 2011], there were differences. No AcO^- was detected in the stream or hyporheic water above the detection limit of 0.01 mg L^{-1}. Both Cl^- and Br^- were present before the experiment, but did not vary between stream and hyporheic waters or among wells (Table 1). Relative to the previous study, the background DOC conditions

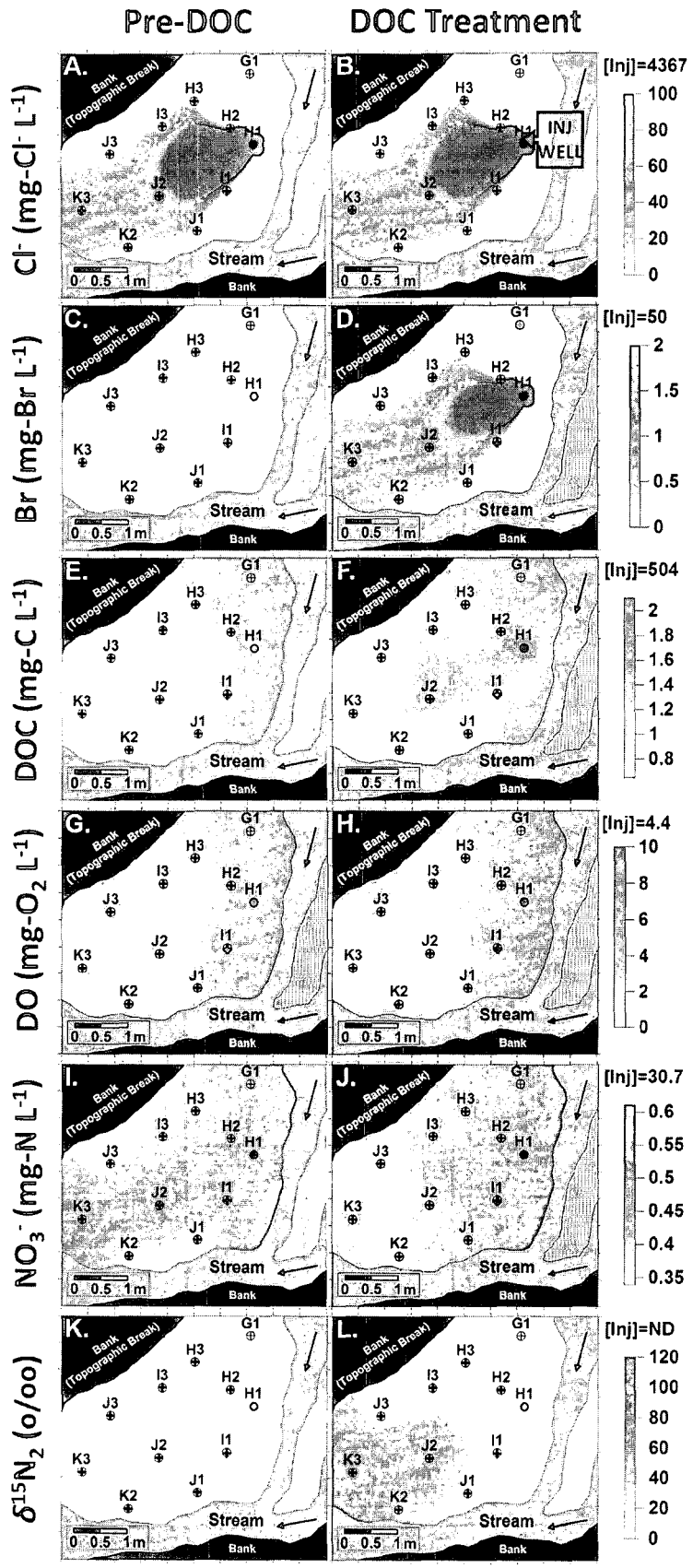

Figure 4. Spatial biogeochemical and $\delta^{15}N$ signatures during steady state Pre-DOC and DOC augmentation periods of the experiment. Reported values are the means for each period (n = 5).

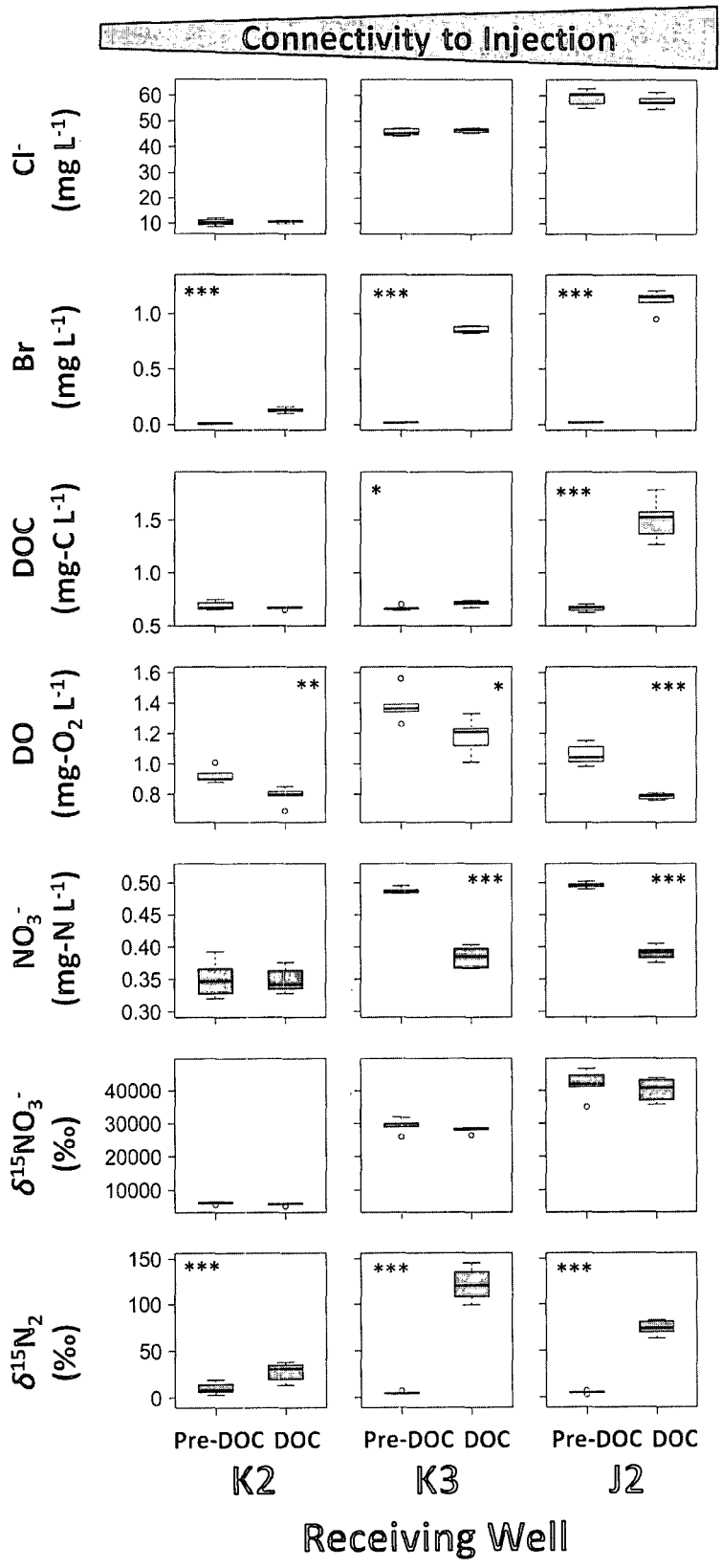

Figure 5. Change in solute concentrations for the Pre-DOC and DOC treatment periods in receiving wells. K2, K3, and J3 demonstrate steady state conditions and are sorted from left to right by increasing levels of connectivity to injection. Note that asterisks denote *t* test significant difference of means at $p < 0.05$ (one asterisk), $p < 0.01$ (two asterisks), and $p < 0.001$ (three asterisks) with df = 4.

Table 2. Steady State DOC Augmentation Period Transport Times, Well Hydrologic Connectivity, and Solute Responses for the Three Wells Hydrologically Connected to H1[a]

Hyporheic Condition	Location		
	K2	K3	J2
Connectivity to injection, D (–)	0.002	0.009	0.013
Median transport time from injection (h)	11.3	13.3	9.8
NO_3^- (mg N L^{-1})			
Background	0.35	0.43	0.41
Pre-DOC	0.35	0.49	0.50
With DOC			
Predicted, S	0.40	0.73	0.76
Observed	0.35	0.38	0.39
Retention	−0.05	−0.35	−0.37
DO (mg O_2 L^{-1})			
Background	0.70	1.31	0.88
Pre-DOC	0.93	1.38	1.06
With DOC			
Predicted, S	0.80	1.34	0.92
Observed	0.79	1.18	0.79
Retention	−0.01	−0.16	−0.13
Acetate (mg AcO^- L^{-1})			
Background	<0.01	<0.01	<0.01
Pre-DOC	<0.01	<0.01	<0.01
With DOC			
Predicted, S	0.80	4.77	6.36
Observed	<0.01	<0.01	<0.01
Retention	−0.80	−4.77	−6.36

[a]Solute background values are means (n = 3); Pre-DOC and DOC period values are means (n = 5).

were lower in stream and hyporheic waters and a strong nitrification region at the head of the hyporheic flowpaths was not present.

3.2. Solute Transport and Retention: Pre-DOC Addition

[24] Four of the nine downgradient wells were hydrologically connected to the H1 well injection site as determined by a significant increase ($p < 0.05$; t test; df = 4) in Cl^- during the first Pre-DOC injection plateau period (H2, J2, K2, K3; Figures 4 and 5). The steady state hydrologic connectivity (D) to the injection was 0.013 at J2, 0.0020 at K2, and 0.0090 at K3 (Table 2). (Note that the tracer injection rate was very low and was diluted into a large volume of hyporheic water flowing through the gravel bar. Still, the relatively high concentration of conservative and ^{15}N tracers resulted in distinct breakthroughs, despite the apparent low connectivity). The H2 well was connected to the injection well, but the level of connectivity varied between Pre-DOC and DOC periods thereby failing the experimental assumption of steady state flow dynamics between the experimental injection periods as shown in section 3.3. The specific conductivity did not vary significantly between Pre-DOC and DOC periods in the other wells (data not shown but see Cl^- in Figures 4a and 4b). Nominal flowpath lengths from the injection site to the receiving wells ranged from 2.18 m (J2) to 3.66 m (K3). The median hyporheic transport times from the injection site to J2, K2, and K3 were 9.8, 11.3, and 13.3 h, respectively (Table 2).

[25] The Cl^- connectivity consistently corresponded with the amount of $^{15}NO_3^-$ reaching the receiving wells ($\delta^{15}NO_3^-$ ‰ = 721.8 * [Cl^- mg L^{-1}] − 2248, r^2 = 0.999, n = 30), so the $^{15}NO_3^-$ tracer spatial plume is the same as the Cl^- plume (Figure 4). Nitrate concentrations were differentially altered by the $K^{15}NO_3$ addition. The two most connected wells showed increased NO_3^- concentration (J2 increased from 0.41 to 0.50 mg N L^{-1} and K3 increased from 0.43 to 0.49 mg N L^{-1}) and there was no change in the least connected well K2 (Table 2). The DOC in three connected wells was lower than background conditions. During this period no AcO^- was detected in any of the repeated sampling rounds (Table 2). $^{15}NO_3^-$ tracer enrichment and $^{15}N_2$ production via denitrification were also detected at significant but varying levels in each of the receiving wells (Figures 4 and 5).

3.3. Solute Transport and Retention: Post-DOC Addition

[26] The steady state conditions of $^{15}NO_3^-$ and Cl^- tracer addition was confirmed as we detected no significant differences ($p > 0.05$; t test, df = 4; Figure 5) between the Pre-DOC and DOC Cl^- concentrations at 3 of the 4 connected wells (J2, K2, K3). Well H2 had a significantly higher Cl^- concentration and $^{15}NO_3^-$ enrichment during the DOC period compared to the Pre-DOC period (see auxiliary material Figure S1).[1] Therefore, H2 is not used for comparison between Pre-DOC and DOC treatment periods of the experiment. Of the connected wells, H2 is located adjacent and closest to the injection site (nominal flowpath length = 0.67 m; Figure 4). The second conservative tracer, Br^-, injected with the AcO^- showed the same dilution and downgradient tracer plume behavior as the Cl^- tracer. The injected AcO^- during the DOC addition period formed a plume from the injection site that behaved similar to the conservative tracers (Figure 4). However, the elevated total DOC concentrations did not persist along the flowpaths and were near Pre-DOC conditions at the most distal downgradient receiving well, K2. Accounting for the AcO^- injected into the hyporheic zone and dilution along the flowpaths to each well showed that all of the AcO^- was retained in the hyporheic zone, with as much as 6.36 mg AcO^- L^{-1} being retained along flowpath between wells H1 and J2 (Table 2).

[27] The DO, NO_3^-, and $\delta^{15}N_2$ conditions changed significantly during the DOC addition. The DO in the receiving wells all showed significantly decreased concentrations under elevated labile DOC conditions creating more anoxic conditions in the three receiving wells ($p < 0.05$; t test; df = 4; Figure 5). The mean NO_3^- concentration decreased in all three receiving wells, with highly significant decreases in NO_3^- seen in the two most connected wells ($p < 0.001$ for K3 and J2; Figure 5). This decrease in NO_3^- resulted in overall NO_3^- conditions lower than the background conditions, and after accounting for dilution showed that NO_3^- was retained along the flowpaths at levels between 0.05 and 0.37 mg N L^{-1}. The $\delta^{15}NO_3^-$ enrichment did not vary significantly following the addition of AcO^-, but the $\delta^{15}N_2$ signature increased significantly in all receiving wells with

[1]Auxiliary material is available in the HTML. doi:10.1029/2011JG001730.

$\delta^{15}N_2$ enrichment increasing up to 26.1 times that of the Pre-DOC levels ($p < 0.001$; t test; df = 4; Figure 5).

4. Discussion

[28] This study demonstrates that labile DOC limits denitrification along hyporheic flowpaths and that NO_3^- losses can be attributed in part to denitrification in this hyporheic zone. The tracing of the denitrification pathway of $^{15}NO_3^-$ to $^{15}N_2$ under ambient and elevated AcO^- (as labile DOC) conditions confirm earlier theoretical- and observation-based conclusions regarding the role of hyporheic DOC quantity and quality on denitrification dynamics in hyporheic systems [*Hedin et al.*, 1998; *Baker et al.*, 1999; *Hill et al.*, 2000; *Sobczak and Findlay*, 2002].

[29] The hyporheic conditions and steady state experimental design allowed us to evaluate our hypotheses about the role of labile DOC in hyporheic denitrification (Figure 2). The post-DOC conditions clearly show that the addition of labile DOC to this hyporheic zone increased metabolic processing rates downgradient of the addition such that the additional labile DOC was utilized and removed rapidly (Figure 4). Utilization of labile DOC stimulated additional aerobic respiration as seen in the increased DO deficit conditions (Figure 5). Consequently, the increased anaerobic conditions and elevated supply of carbon substrate, lead to significant increases in denitrification rates. Overall, the addition of labile DOC resulted in a significant increase in the total NO_3^- mass removed by this gravel bar hyporheic zone (Figure 5).

4.1. Hyporheic Zone as a Stream DOC Sink

[30] This study shows that the hyporheic zone is a sink for stream DOC and that within the hyporheic zone, the availability of labile DOC is a critical factor controlling denitrification. We observed a DOC gradient across the gravel bar flowpaths. At the head of the gravel bar, the hyporheic water DOC concentrations are similar to the DOC of surface waters, but hyporheic DOC concentration consistently declined along the flowpaths (Figure 4). Spatial declines of hyporheic DOC along flowpaths are consistently seen in gravel bar hyporheic investigations where the major source of hyporheic DOC is stream water [e.g., *Vervier and Naiman*, 1992; *Findlay et al.*, 1993]. We also know that, in this gravel bar, the lability of DOC declined along the flowpath and at a rate greater than the decline of total DOC [*Zarnetske et al.*, 2011]. Declines in labile DOC along hyporheic flowpaths have been previously documented in natural and experimental hyporheic systems where DOC quality was measured [e.g., *Sobczak and Findlay*, 2002; *Sobczak et al.*, 2003]. For example, when bioavailable nitrogen is available, labile DOC will decline along riparian and hyporheic flowpaths due to microbial productivity and assimilation [*Sobczak et al.*, 1998; *Sobczak and Findlay*, 2002] and increased metabolism [*Baker et al.*, 2000].

[31] A portion of the DOC advected through the gravel bar is used for microbial aerobic and anaerobic respiration, as shown by the rapid depletion of DO and the ambient levels of denitrification occurring along the flowpaths (Figures 4 and 5). We also know that despite the large addition of AcO^- to this gravel bar, no above-background AcO^- concentrations were detected at any downgradient points before or during the AcO^- addition. The 100% retention of the AcO^- across a 24 h plateau injection period (i.e., the DOC, as AcO^-, uptake capacity was not achieved) combined with the known low sorption potential and high solubility of AcO^- [e.g., *Baker et al.*, 1999] indicates that in this hyporheic zone, metabolism is strongly limited by DOC supply even under the elevated DOC conditions of the experiment. The controlled experimental observations of DOC limitation on hyporheic metabolism in this study mirror the findings of *Jones* [1995] and *Baker et al.* [2000], who observed that natural variations in stream-sourced DOC supply correlated with hyporheic metabolism and N transformation rates.

4.2. Labile DOC Supply Controls Hyporheic NO_3^- Dynamics

[32] The hyporheic denitrification rates are DOC substrate limited in this gravel bar as documented along the extended flowpaths leading to wells J2, K2, and K3, where all other conditions for denitrification are present except for a sufficient source of labile DOC to serve as an electron donor. This was proven under controlled, steady state conditions where just a change in the labile DOC availability resulted in more extensive anaerobic conditions and increased denitrification rates (both NO_3^- concentrations decreased and $\delta^{15}N_2$ signature increased significantly (Figures 4 and 5)).

[33] The hyporheic DOC and NO_3^- dynamics fit the conceptual model of *Findlay* [1995], which hypothesizes that the influence of the hyporheic zone at the reach scale is a function of two variables: the rate of hydrologic exchange in and out of the hyporheic zone and the rate of biogeochemical processes in the hyporheic zone. In this system, we see that denitrification is limited by the amount of labile DOC supplied via hydrologic exchange from the DOC-rich surface waters. No lateral hillslope or groundwater inflow has been detected at this gravel bar site. Thus, surface water is the primary source of DOC to this hyporheic zone at summer low flow. Consequently, denitrification in this system will vary primarily as a function of the quantity and quality of the DOC in the surface water and the hydrologic conditions promoting hyporheic exchange across the gravel bar. During a prior investigation on the same gravel bar [*Zarnetske et al.*, 2011], the hyporheic zone had a much greater NO_3^- removal efficiency with approximately 99% of the NO_3^- removed along flowpaths traversing the gravel bar versus only 57% in this study. During the previous study, hydrologic exchange conditions were similar (i.e., head gradient, hydraulic conductivity, and residence time) as were the ambient stream NO_3^- concentrations (0.54 mg L^{-1} and 0.61 mg L^{-1}, respectively), but a key difference was that stream DOC concentration entering the hyporheic zone was much higher: 3.01 mg L^{-1} in the previous study versus 1.94 mg L^{-1} in the current study. The larger flux of DOC to the head of the gravel bar during the earlier study also stimulated greater DO consumption rates. These higher DO consumption rates lead to the development of anoxic conditions occurring over shorter flowpath lengths than the present study. Therefore, a larger portion of the hyporheic zone had reducing conditions conducive to denitrification in the study by *Zarnetske et al.* [2011]. However, after adding the labile DOC source to the hyporheic zone in this study we see that the gravel bar becomes more anoxic and NO_3^- removal efficiency almost

doubled from the Pre-DOC to the DOC periods (Table 2 and Figure 5).

[34] The addition of the labile DOC along midflowpaths also changed the transport of advected stream DOC through the gravel bar. There were higher total DOC concentrations in receiving wells J2 and K3 during the acetate addition period (Figure 5). The acetate addition did not directly add to the measured total DOC concentrations as no acetate was recovered in the down gradient wells. However, the acetate may have indirectly increased downgradient total DOC concentrations in two ways. First, the acetate is preferentially consumed over many other stream-sourced DOC compounds [*Hall and Meyer*, 1998], which could decrease the uptake rate of stream-sourced DOC. Second, the physical adsorption of hyporheic DOC is concentration dependent [*Findlay and Sobczak*, 1996] and leads to DOC immobilization [*Fiebig and Lock*, 1991]. The subsurface acetate addition may have filled many of the DOC sorption sites with acetate. Thus decreasing the number of available DOC sorption sites along the flowpaths, and decreasing the uptake rate of stream-sourced DOC. Together the preferential uptake of acetate and decrease in available DOC sorption sites, in effect, would shunt the stream-sourced DOC further down the flowpaths resulting in the higher total DOC concentrations in J2 and K3 during the acetate injection period.

[35] We conclude that, with sufficient upgradient supply of labile DOC entering hyporheic environments, the hyporheic zone can play a very significant role in regulating downstream NO_3^- export in Drift Creek. To demonstrate this point, we compare ambient NO_3^- removal rates to the DOC augmented removal rates at the gravel bar site. A calibrated groundwater flow model of the hyporheic zone site shows a minimum of 226 L m^{-2} d^{-1} of hyporheic exchange flow occurs under the summer low-flow conditions of the DOC experiment [*Zarnetske*, 2011]. Given this hydrologic exchange flow and the background observed NO_3^- retention rates, the NO_3^- mass removal rate at this gravel bar at this time is 218 kg ha^{-1} yr^{-1}. This removal rate is within the range of previous surface water–groundwater exchange studies (e.g., 10–39 kg ha^{-1} yr^{-1} [*Lowrance et al.*, 1997]; up to 6600 kg ha^{-1} yr^{-1} [*Hedin et al.*, 1998]). In comparison to the NO_3^- and DOC values seen in these previous studies, the ambient NO_3^- and DOC in our system was an order of magnitude lower for both N and C constituents. The decreased availability of NO_3^- and DOC alone can limit the potential for total NO_3^- removal via denitrification compared to the previous investigations. However, by artificially increasing only the supply of labile hyporheic DOC to our receiving wells (i.e., not the entire gravel bar), we were able to increase the NO_3^- removal rate by 303 kg ha^{-1} yr^{-1}, to a total of 521 kg ha^{-1} yr^{-1}. This is an increase of 139% above background removal rates.

[36] The injection of labile DOC in this experimental gravel bar is akin to groundwater–surface water environments where a DOC-rich groundwater or riparian flowpath converges with other hyporheic flowpaths. *Hedin et al.* [1998] and *Hill et al.* [2000] observed high denitrification rates where hydrologic conditions promoted mixing of DOC-rich groundwaters with DOC-poor waters that contained NO_3^-. Therefore, the formation of these denitrification hot spots is governed by the complex groundwater hydraulics that mix waters containing DOC and NO_3^- [*McClain et al.*, 2003]. In this gravel bar hyporheic zone, the ambient DOC gradient is the result of an imbalance between the hydrologic transport and biogeochemical reaction kinetics: the advected supply rate is less than the biochemical demand rate for labile DOC. By experimentally manipulating the labile DOC gradient with an acetate addition we altered the balance between transport and reaction kinetics and created a denitrification hot spot and altered total DOC transport in this hyporheic zone.

[37] This experiment also indicates that anthropogenic (intentional and unintentional) or natural additions of labile DOC to a hyporheic system will facilitate greater denitrification if NO_3^- supply is not limiting. Similar to groundwater remediation practices (e.g., denitrification walls, in the sense of *Schipper and Vojvodic-Vukovic* [1998]), strategic additions of a labile DOC source to the near stream environment could mitigate NO_3^- flux into a stream system [*Pfenning and McMahon*, 1997; *Hedin et al.*, 1998], but that would require extensive understanding of the complex hydrologic flowpaths and flow rates leading to the denitrification sites.

5. Conclusions

[38] We showed that hyporheic environments are an important sink for both DOC and nitrate in freshwater ecosystems and that the fate of nitrate, in this case denitrification, is tightly coupled to C dynamics. The in situ steady state labile DOC and $^{15}NO_3^-$ addition experiment definitively showed that denitrification is occurring in the hyporheic zone of this upland agricultural stream and that the availability of labile C strongly limits the overall denitrification potential. We echo *Gruber and Galloway* [2008]: C and N cycles are coupled in river systems and they should be evaluated and modeled as coupled processes. The use of total DOC in hyporheic denitrification models is likely to overestimate denitrification potentials, especially if all the DOC is considered available for microbial processes. This study indicates that future hyporheic denitrification investigations should measure and account for the labile fraction of DOC and not just the total DOC.

[39] **Acknowledgments.** Support for this project was primarily provided by a NSF Ecosystem Informatics IGERT fellowship (grant DGE-0333257) to J.P.Z.; research grants from the OSU Institute for Water and Watersheds and a North American Benthological Society Endowment Fund to J.P.Z.; and NSF grants EAR-0409534 and EAR-0409591 to R.H., S.M.W., and M.A.B. Additional support was provided by the Hollis M. Dole Environmental Geology Fund at OSU. Any opinions, findings, and conclusions or recommendations expressed in this material are those of the authors and do not necessarily reflect the views of NSF. We thank the Harry Klopfenstein Farm for generously granting access to the Drift Creek research sites. Special thanks to V. Adams, P. Zarnetske, and J. Yin for field assistance and C. Jones and K. Motter of CCAL and OSU IWW Collaboratory for help with analyzing general water chemistry.

References

Alexander, R. B., R. A. Smith, and G. E. Schwarz (2000), Effect of stream channel size on the delivery of nitrogen to the Gulf of Mexico, *Nature*, *403*, 758–761, doi:10.1038/35001562.

Anderson, J. K., S. M. Wondzell, M. N. Gooseff, and R. Haggerty (2005), Patterns in stream longitudinal profiles and implications for hyporheic exchange flow at the H.J. Andrews Experimental Forest, Oregon, USA, *Hydrol. Processes*, *19*, 2931–2949, doi:10.1002/hyp.5791.

Arango, C. P., J. L. Tank, J. L. Schaller, T. V. Royer, M. J. Bernot, and M. B. David (2007), Benthic organic carbon influences denitrification in

streams with high nitrate concentration, *Freshwater Biol.*, *52*, 1210–1222, doi:10.1111/j.1365-2427.2007.01758.x.

Baker, M. A., and P. Vervier (2004), Hydrological variability, organic matter supply and denitrification in the Garonne River ecosystem, *Freshwater Biol.*, *49*, 181–190, doi:10.1046/j.1365-2426.2003.01175.x.

Baker, M. A., C. N. Dahm, and H. M. Valett (1999), Acetate retention and metabolism in the hyporheic zone of a mountain stream, *Limnol. Oceanogr.*, *44*, 1530–1539, doi:10.4319/lo.1999.44.6.1530.

Baker, M. A., H. M. Valett, and C. N. Dahm (2000), Organic carbon supply and metabolism in a shallow groundwater ecosystem, *Ecology*, *81*, 3133–3148, doi:10.1890/0012-9658(2000)081[3133:OCSAMI]2.0.CO;2.

Böhlke, J. K., J. W. Harvey, and M. A. Voytek (2004), Reach-scale isotope tracer experiment to quantify denitrification and related processes in a nitrate-rich stream, midcontinent United States, *Limnol. Oceanogr.*, *49*, 821–838, doi:10.4319/lo.2004.49.3.0821.

Böhlke, J. K., R. C. Antweiler, J. W. Harvey, A. E. Laursen, L. K. Smith, R. L. Smith, and M. A. Voytek (2009), Multi-scale measurements and modeling of denitrification in streams with varying flow and nitrate concentration in the upper Mississippi River basin, USA, *Biogeochemistry*, *93*, 117–141, doi:10.1007/s10533-008-9282-8.

Chapelle, F. H., and P. M. Bradley (1996), Microbial acetogenesis as a source of organic acids in ancient Atlantic coastal plain sediments, *Geology*, *24*, 925–928, doi:10.1130/0091-7613(1996)024<0925:MAAASO>2.3.CO;2.

Clilverd, H. M., J. B. Jones, and K. Kielland (2008), Nitrogen retention in the hyporheic zone of a glacial river in interior Alaska, *Biogeochemistry*, *88*, 31–46, doi:10.1007/s10533-008-9192-9.

Drake, H. L. (1994), Introduction to acetogenesis, in *Acetogenesis*, edited by H. L. Drake, pp. 3–61, Chapman and Hall, New York.

Duff, J. H., and F. J. Triska (1990), Denitrification in sediments from the hyporheic zone adjacent to a small forested stream, *Can. J. Fish. Aquat. Sci.*, *47*, 1140–1147, doi:10.1139/f90-133.

Duff, J. H., and F. J. Triska (2000), Nitrogen biogeochemistry and surface-subsurface exchange in streams, in *Streams and Ground Waters*, edited by J. B. Jones and P. J. Mulholland, pp. 197–220, Academic, San Diego, Calif., doi:10.1016/B978-012389845-6/50009-0

Fiebig, D. M., and M. A. Lock (1991), Immobilization of dissolved organic matter from groundwater discharging through the stream bed, *Freshwater Biol.*, *26*, 45–55, doi:10.1111/j.1365-2427.1991.tb00507.x.

Findlay, S. (1995), Importance of surface-subsurface exchange in stream ecosystems: The hyporheic zone, *Limnol. Oceanogr.*, *40*, 159–164, doi:10.4319/lo.1995.40.1.0159.

Findlay, S., and W. V. Sobczak (1996), Variability in removal of dissolved organic carbon in hyporheic sediments, *J. North Am. Benthol. Soc.*, *15*, 35–41, doi:10.2307/1467431.

Findlay, S., D. Strayer, C. Goumbala, and K. Gould (1993), Metabolism of streamwater dissolved organic-carbon in the shallow hyporheic zone, *Limnol. Oceanogr.*, *38*, 1493–1499, doi:10.4319/lo.1993.38.7.1493.

Fisher, S. G., and G. E. Likens (1973), Energy flow in Bear Brook, New Hampshire: An integrative approach to stream ecosystem metabolism, *Ecol. Monogr.*, *43*, 421–439, doi:10.2307/1942301.

Gruber, N., and J. N. Galloway (2008), An Earth-system perspective of the global nitrogen cycle, *Nature*, *451*, 293–296, doi:10.1038/nature06592.

Hall, R. O., Jr., and J. L. Meyer (1998), The trophic significance of bacteria in a detritus-based stream food web, *Ecology*, *79*, 1995–2012, doi:10.1890/0012-9658(1998)079[1995:TTSOBI]2.0.CO;2.

Hamilton, S. K., and N. E. Ostrom (2007), Measurement of the stable isotope ratio of dissolved N-2 in N-15 tracer experiments, *Limnol. Oceanogr. Methods*, *5*, 233–240, doi:10.4319/lom.2007.5.233.

Hedin, L. O., J. C. von Fischer, N. E. Ostrom, B. P. Kennedy, M. G. Brown, and G. P. Robertson (1998), Thermodynamic constraints on nitrogen transformations and other biogeochemical processes at soil-stream interfaces, *Ecology*, *79*, 684–703, doi:10.1890/0012-9658(1998)079[0684:TCONAO]2.0.CO;2].

Hill, A. R., C. F. Labadia, and K. Sanmugadas (1998), Hyporheic zone hydrology and nitrogen dynamics in relation to the streambed topography of a N-rich stream, *Biogeochemistry*, *42*, 285–310, doi:10.1023/A:1005932528748.

Hill, A. R., K. J. Devito, S. Campagnolo, and K. Sanmugadas (2000), Subsurface denitrification in a forest riparian zone: Interactions between hydrology and supplies of nitrate and organic carbon, *Biogeochemistry*, *51*, 193–223, doi:10.1023/A:1006476514038.

Holmes, R. M., S. G. Fisher, and N. B. Grimm (1994), Parafluvial nitrogen dynamics in a desert stream ecosystem, *J. North Am. Benthol. Soc.*, *13*, 468–478, doi:10.2307/1467844.

Holmes, R. M., J. B. Jones, S. G. Fisher, and N. B. Grimm (1996), Denitrification in a nitrogen-limited stream ecosystem, *Biogeochemistry*, *33*, 125–146, doi:10.1007/BF02181035.

Jones, J. B. (1995), Factors controlling hyporheic respiration in a desert stream, *Freshwater Biol.*, *34*, 91–99, doi:10.1111/j.1365-2427.1995.tb00426.x.

Kaplan, L. A., and J. D. Newbold (2000), Surface and subsurface dissolved organic carbon, in *Streams and Ground Waters*, edited by J. B. Jones and P. J. Mulholland, pp. 237–258, Academic, San Diego, Calif., doi:10.1016/B978-012389845-6/50011-9

Lowrance, R., et al. (1997), Water quality functions of riparian forest buffer systems in the Chesapeake Bay watersheds, *Environ. Manage. N. Y.*, *21*, 687–712, doi:10.1007/s002679900060.

McClain, M. E., et al. (2003), Biogeochemical hot spots and hot moments at the interface of terrestrial and aquatic ecosystems, *Ecosystems*, *6*, 301–312, doi:10.1007/s10021-003-0161-9.

Montgomery, D. R., and J. M. Buffington (1997), Channel-reach morphology in mountain drainage basins, *Geol. Soc. Am. Bull.*, *109*, 596–611, doi:10.1130/0016-7606(1997)109<0596:CRMIMD>2.3.CO;2.

Mulholland, P. J., H. M. Valett, J. R. Webster, S. A. Thomas, L. W. Cooper, S. K. Hamilton, and B. J. Peterson (2004), Stream denitrification and total nitrate uptake rates measured using a field ^{15}N tracer addition approach, *Limnol. Oceanogr.*, *49*, 809–820, doi:10.4319/lo.2004.49.3.0809.

Mulholland, P. J., et al. (2008), Stream denitrification across biomes and its response to anthropogenic nitrate loading, *Nature*, *452*, 202–205, doi:10.1038/nature06686.

Peterson, B. J., et al. (2001), Control of nitrogen export from watersheds by headwater streams, *Science*, *292*, 86–90, doi:10.1126/science.1056874.

Pfenning, K. S., and P. B. McMahon (1997), Effect of nitrate, organic carbon, and temperature on potential denitrification rates in nitrate-rich riverbed sediments, *J. Hydrol.*, *187*, 283–295, doi:10.1016/S0022-1694(96)03052-1.

Schipper, L., and M. Vojvodic-Vukovic (1998), Nitrate removal from groundwater using a denitrification wall amended with sawdust: Field trial, *J. Environ. Qual.*, *27*, 664–668, doi:10.2134/jeq1998.00472425002700030025x.

Seitzinger, S. P. (1988), Denitrification in freshwater and coastal marine ecosystems: Ecological and geochemical significance, *Limnol. Oceanogr.*, *33*, 702–724, doi:10.4319/lo.1988.33.4_part_2.0702.

Seitzinger, S., J. A. Harrison, J. K. Böhlke, A. F. Bouwman, R. Lowrance, B. Peterson, C. Tobias, and G. Van Drecht (2006), Denitrification across landscapes and waterscapes: A synthesis, *Ecol. Appl.*, *16*, 2064–2090, doi:10.1890/1051-0761(2006)016[2064:DALAWA]2.0.CO;2.

Sigman, D. M., M. A. Altabet, R. Michener, D. C. McCorkle, B. Fry, and R. M. Holmes (1997), Natural abundance-level measurement of the nitrogen isotopic composition of oceanic nitrate: An adaptation of the ammonia diffusion method, *Mar. Chem.*, *57*, 227–242, doi:10.1016/S0304-4203(97)00009-1.

Smith, L. K., M. A. Voytek, J. K. Böhlke, and J. W. Harvey (2006), Denitrification in nitrate-rich streams: Application of N_2:Ar and ^{15}N tracer methods in intact cores, *Ecol. Appl.*, *16*, 2191–2207, doi:10.1890/1051-0761(2006)016[2191:DINSAO]2.0.CO;2.

Sobczak, W. V., and S. Findlay (2002), Variation in bioavailability of dissolved organic carbon among stream hyporheic flowpaths, *Ecology*, *83*, 3194–3209, doi:10.1890/0012-9658(2002)083[3194:VIBODO]2.0.CO;2.

Sobczak, W. V., L. O. Hedin, and M. J. Klug (1998), Relationships between bacterial productivity and organic carbon at a soil-stream interface, *Hydrobiologia*, *386*, 45–53, doi:10.1023/A:1003583813445.

Sobczak, W. V., S. Findlay, and S. Dye (2003), Relationships between DOC bioavailability and nitrate removal in an upland stream: An experimental approach, *Biogeochemistry*, *62*, 309–327, doi:10.1023/A:1021192631423.

Storey, R. G., D. D. Williams, and R. R. Fulthorpe (2004), Nitrogen processing in the hyporheic zone of a pastoral stream, *Biogeochemistry*, *69*, 285–313, doi:10.1023/B:BIOG.0000031049.95805.ec.

Swank, W. T., and W. H. Caskey (1982), Nitrate depletion in a second-order mountain stream, *J. Environ. Qual.*, *11*, 581–584.

Valett, H. M., et al. (1996), Parent lithology, surface-groundwater exchange, and nitrate retention in headwater streams, *Limnol. Oceanogr.*, *41*, 333–345, doi:10.4319/lo.1996.41.2.0333.

Vervier, P., and R. J. Naiman (1992), Spatial and temporal fluctuations of dissolved organic-carbon in subsurface flow of the Stillaguamish River (Washington, USA), *Arch. Hydrobiol.*, *123*, 401–412.

Woessner, W. W. (2007), Building a compact, low-cost, and portable peristaltic sampling pump, *Ground Water*, *45*, 795–797, doi:10.1111/j.1745-6584.2007.00346.x.

Wondzell, S. M. (2011), The role of the hyporheic zone in stream networks, *Hydrol. Processes*, *25*, 3525–3532, doi:10.1002/hyp.8119.

Wondzell, S. M., and F. J. Swanson (1996), Seasonal and storm dynamics of the hyporheic zone of a 4th-order mountain stream. II: Nitrogen cycling, *J. North Am. Benthol. Soc.*, *15*, 20–34, doi:10.2307/1467430.

Zarnetske, J. P. (2011), Hydrological and biogeochemical dynamics of nitrate production and removal at the stream–ground water interface, Ph.D. thesis, 173 pp., Oreg. State Univ., Corvallis.

Zarnetske, J. P., R. Haggerty, S. M. Wondzell, and M. A. Baker (2011), Dynamics of nitrate production and removal as a function of residence time in the hyporheic zone, *J. Geophys. Res.*, *116*, G01025, doi:10.1029/2010JG001356.

M. A. Baker, Department of Biology, Utah State University, 5305 Old Main Hill, Logan, UT 84322, USA.

R. Haggerty, Department of Geosciences, Oregon State University, 104 Wilkinson Hall, Corvallis, OR 97330-5506, USA.

S. M. Wondzell, Pacific Northwest Research Station, Olympia Forestry Sciences Lab, 3625 93rd Ave. SW, Olympia, WA 98512, USA.

J. P. Zarnetske, School of Forestry and Environmental Studies, Yale University, 195 Prospect St., New Haven, CT 06513, USA. (jay.zarnetske@yale.edu)